Laser and Particle Beams (2014), *32*, 495–500.

doi:10.1017/S0263034614000433

Laser driven electron acceleration in a CNT embedded gas jet target

ASHOK KUMAR,[1] DEEPAK DAHIYA,[2] AND V. K. TRIPATHI[2]

[1]Department of Physics, AIAS, Amity University, Noida, India
[2]Department of Physics, IIT Delhi, New Delhi, India

(Received 28 March 2014; Accepted 9 July 2014)

Abstract

The bubble regime acceleration of electrons by a short pulse laser in a carbon nanotube (CNT) embedded plasma is investigated, employing two-dimensional Particle-in-Cell simulations. The laser converts the CNT placed on the laser axis into dense plasma and expels the electrons out, to form a co-moving positive charged sheet inside the bubble. The additional field generated due to sheet enhances the energy of the monoenergetic bunch by about 5% and their number by 5–20%. For a typical 40 fs, 7.5×10^{19} Wcm^{-2} pulse in an underdense plasma of density n_0, CNT of thickness 25 nm and electron density $30n_0$, produces a monoenergetic bunch of 115 MeV with 5% energy spread. When CNT density is raised to $90n_0$, the energy gain, energy spread and accelerated charge increases further. The analytical framework supports these features.

Keywords: Electron acceleration; Laser; Wakefield acceleration

1. INTRODUCTION

The laser driven electron acceleration is an important area of research due to its wide ranging applications, from fast ignition fusion to X-ray and magnetic field generation (Bagchi *et al.*, 2011; Hora, 2009; Joshi, 2007; Liu *et al.*, 2012; Tajima & Dawson, 1979). Improvements in various key factors such as electron bunch energy, number of particles accelerated, and low energy spread are essential for making it attractive for various applications (Faure *et al.*, 2004; Miura *et al.*, 2005; Kalmykov *et al.*, 2009; Mirzanejhad *et al.*, 2010; Kostyukov *et al.*, 2004; Yi *et al.*, 2013, Upadhyay *et al.*, 2013; Jokar & Eslami, 2012). In the last two decades, many experiments and simulations have been performed in order to understand the physics of the electron acceleration in underdense plasma. One of the schemes, laser-wakefield acceleration (LWFA) has become a practical reality with numerous recent experimental results (Mangles *et al.*, 2004; Geddes *et al.*, 2004; Faure *et al.*, 2004; Leemans *et al.*, 2006; Hafz *et al.*, 2008; Lu *et al.*, 2006; Jha *et al.* 2013). A short laser pulse of duration equal to the plasma period excites a large amplitude plasma wave in its wake with phase velocity equal to the group velocity of the laser. Electrons trapped in the proper phase of the plasma wave are accelerated to very high energies by the axial electric field of the wave. Several methods have been proposed for better electron trapping and enhancement in the electron bunch energy and charge (Xu *et al.*, 2010; Dahiya *et al.*, 2010; Faure *et al.*, 2006; Hidding *et al.*, 2010; Vieira *et al.*, 2011; 2012; Esarey *et al.*, 1997; Umstadter *et al.*, 1996; Hemker *et al.*, 1998).

At relativistically high laser intensity and small spot size, the laser pulse expels all the electrons from the axial region, through axial and radial ponderomotive force. The scenario known as bubble regime has been extensively studied using Particle-in-Cell (PIC) simulations. PIC has allowed analyzing the complex behavior of the bubble scenario in a systematic way, which led to many refinements in the scheme. In many studies, a preformed plasma channel is employed for the efficient laser guiding much beyond the diffraction length and yielded electron beams with narrow energy spread (Rao *et al.*, 2011; Martins *et al.*, 2010; Kumar *et al.*, 2011; Gu *et al.*, 2011). Zhang *et al.* (2012) have studied electron acceleration in a submicron sized cluster-gas targets. Wang *et al.* (2008) have suggested a scheme for better electron injection by using two orthogonally directed laser pulses. Murakami *et al.* (2013) have utilized the extraordinary material and mechanical property of CNT to generate quasimonoenergetic proton beams.

Address correspondence and reprint requests to: Ashok Kumar, Department of Physics, AIAS, Amity University, Noida, UP, 201303, India. E-mail: akumar16@amity.edu

Shen *et al.* (2007) have studied the triggering wave breaking using a nanowire. Ma *et al.* (2006) conjectured the production of attosecond electron bunches by ponderomotive force acceleration along the surface of nanowire. Davoine *et al.* (2009) have reported another injection scheme by modifying the electron's spatial trajectory. Karmakar and Pukhov (2007) have obtained GeV electrons using high-Z materials. Uhm *et al.* (2013) investigated the electron dynamics trapped in a cavity using a theoretical model. Kumar and Tripathi (2012) have developed a bubble regime electron acceleration using Lorentz boosted frame and calculate the energy of the trapped electrons.

In this paper, we develop a model of laser wakefield electron acceleration in the blow out regime in a pre-existing non-uniform plasma channel having a nanotube along the axis. An intense short pulse, with pulse duration of the plasma period ωp, spot size r_0 on the order of $(c/\omega p)$, where c is the speed of light in free space, and normalized amplitude a_0, exerts axial, and radial ponderomotive force on the plasma electrons creating an ion bubble co-moving with the laser pulse. The model and simulations in 2D creates a cylindrical ion bubble with the axis transverse to the direction of pulse propagation. The presence of a nanotube three-dimensional (3D)/sheet (2D) leads to creation of a very thin charged line/sheet layer (with charge density n_{tube} and thickness $\Delta_{\square} << \lambda$, where λ is the wavelength of the laser used) which affect little the overall propagation of laser mode. The bubble radius depends on the laser spot size and laser amplitude and eventually decides the electron energy and its energy spread. The presence of a nanotube augments the charge density by $Z_A n_T$ along the axis, Z_A being the atomic number of the CNT and n_T is the number density. The laser ponderomotive forces expel the CNT electrons, along with the plasma electrons radically outward. In the moving frame, the expelled electrons appear travelling backwards toward the stagnation point which appears as a stagnation line in 2D. The presence of high density ionic sheet modifies the scenario in three ways helpful in the desired goals of electron acceleration. First, the finite ionic sheet along the direction of propagation leads to generation of an additional electric field along the direction of propagation providing an additional pull on the electrons. Second, the inward addition pull toward the axis by the sheet field restricts the momentum spread in the transverse direction leading to bunch directionality. Third, the injection increases the number of accelerated electrons. We calculate addition energy gain of a test electron for a given thickness and density of the sheet and compare the results with PIC simulations.

In Section 2, we provide an analytical background to the CNT aided acceleration. Simulation results are presented in Section 3. The numerical results of the model and simulation results are compared and discussed in Section 4.

2. ANALYSIS

Let us consider a parabolic plasma channel embedded with a nanotube along the propagation axis. In two dimensions, the plasma density can be taken as

$$n = n_0\left(1 + \frac{y^2}{y_0^2}\right) + n_{tube}, \tag{1}$$

$n_{tube} = Z_A N_T$ for $-\Delta/2 < y < \Delta/2$ or 0 otherwise, where Z_A is the charge on one carbon atom, N_T is the number density of carbon atoms inside the tube and Δ is the tube thickness (Fig. 1). In the wake of the pulse, one gets a plasma ion bubble of radius 2R embedded with thin high density charged sheet of length 2R along the axis. A preformed plasma channel assists favorably to the self guiding of a high intensity pulse. The additional electric field due to the trapped ion sheet inside the bubble can be calculated as follows.

Let the laser propagation be in x-direction with origin at the back of the bubble. The charged sheet lies in the x-z plane. Considering an element of charged sheet of length dx' at x' (with $x' = 0$ coinciding with the origin at $x = 0$) the electric field due to this sheet element inside the bubble at distance r can be written as

$$E_r = \left(\frac{n_{tube} e}{2\epsilon_0}\right) r, \quad r < \Delta; \tag{2}$$

$$= \left(\frac{n_{tube} e}{2\epsilon_0 \pi}\right)\left(\frac{\Delta dx'}{r}\right), \quad r > \Delta. \tag{3}$$

The axial and transverse electric field at a point $P(x,y)$ is

$$E_{|\square|} = \int_0^{2R} \frac{Z_A N_T e \Delta}{2\epsilon_0 \pi} \frac{(x - x')}{\{(x - x')^2 + y^2\}^{1/2}} dx'; \tag{4}$$

$$E_{\perp} = \int_0^{2R} \frac{Z_A N_T e \Delta}{2\epsilon_0 \pi} \frac{y}{\{(x - x')^2 + y^2\}^{1/2}} dx'. \tag{5}$$

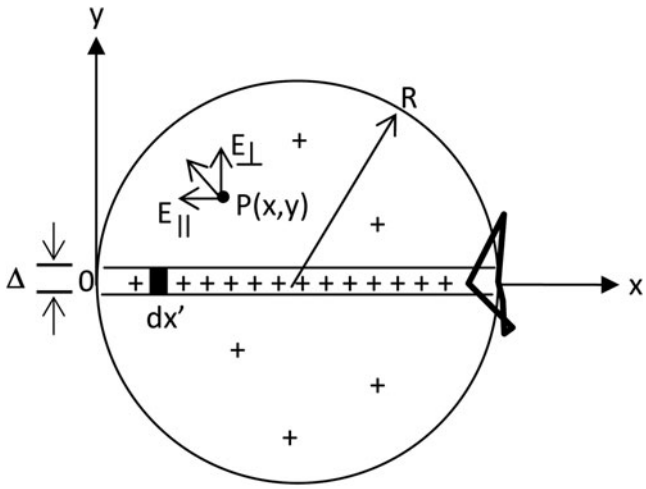

Fig. 1. Schematic of the bubble and embedded CNT. The width of CNT is Δ = 25 nm.

https://doi.org/10.1017/S0263034614000433 Published online by Cambridge University Press

The additional energy gained by an electron due to the axial field by the sheet depends on its transverse distance from the laser axis and is given by

$$KE_{add} = \frac{Z_A N_T e^2 \Delta}{2\epsilon_0 \pi} \int_{\alpha}^{R} \int_{0}^{2R} \frac{(x - x')dx'}{[(x - x')^2 + y^2]^{1/2}} dx, \quad (6)$$

where α is the starting point close to the stagnation point.

3. SIMULATION RESULTS

We simulate the described model using PIC code VORPAL and compare it with the results of a non CNT embedded case of bubble acceleration using standard parameters. A linearly polarized Gaussian laser pulse is launched from the left boundary in the pre-ionized plasma. Moving window is used to simulate 300 μm long plasma systems which contain two bubbles. Physical parameters used in the simulations are as follows: laser wavelength $\lambda = 1\mu m$, normalized peak laser intensity $a_0 = 5$, initial spot size $r_0 = 7\mu m$, pulse duration $\tau_L = 40fs$ (FWHM), uniform background plasma density $n_0 = 1.0 \times 10^{19}\ cm^{-3}$, and $\frac{n_0}{n_c} = 0.01$, number of grids in 2D simulation box $N_x N_y = 1200, 800$ with grid size $N_x = \frac{\lambda}{40}$ and $N_y = \frac{\lambda}{80}$ resulting in physical simulation size of $300 \times 20\ \mu m^2$. Number of macro-particles per cell is 16 in 2D simulations. The presence of a preformed plasma channel keeps the laser pulse self-focused over a sufficient diffraction length. The nanotube of thickness (25 nm) appears as a thin dark line along the laser axis (Fig. 2).

We run a reference simulation without a CNT, calling it case-0, for a typical standard parameters of LWFA and obtain two accelerated electron bunches in the first two bubbles after 600 fs. The energy of the first bunch ranges from 89 MeV to 111 MeV peaking at 100 MeV (Fig. 3a-1). The electron bunch in the second bubble has an energy range from 27 MeV to 46 MeV (Fig. 3a-2). The two bunches are well separated in energy and their energy gap is approximately 43 MeV. The minimum cut-off energy of the second bunch (27 MeV) is well separated

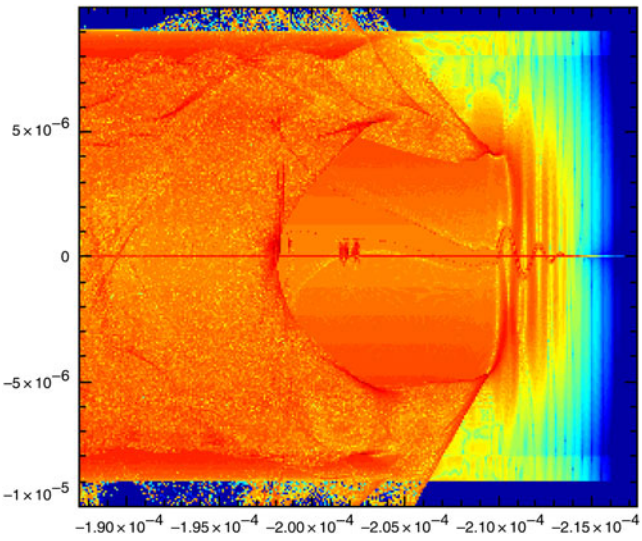

Fig. 2. (Color online) Moving Simulation window showing CNT at the axis. The dimensions are (30 μm × 20 μm).

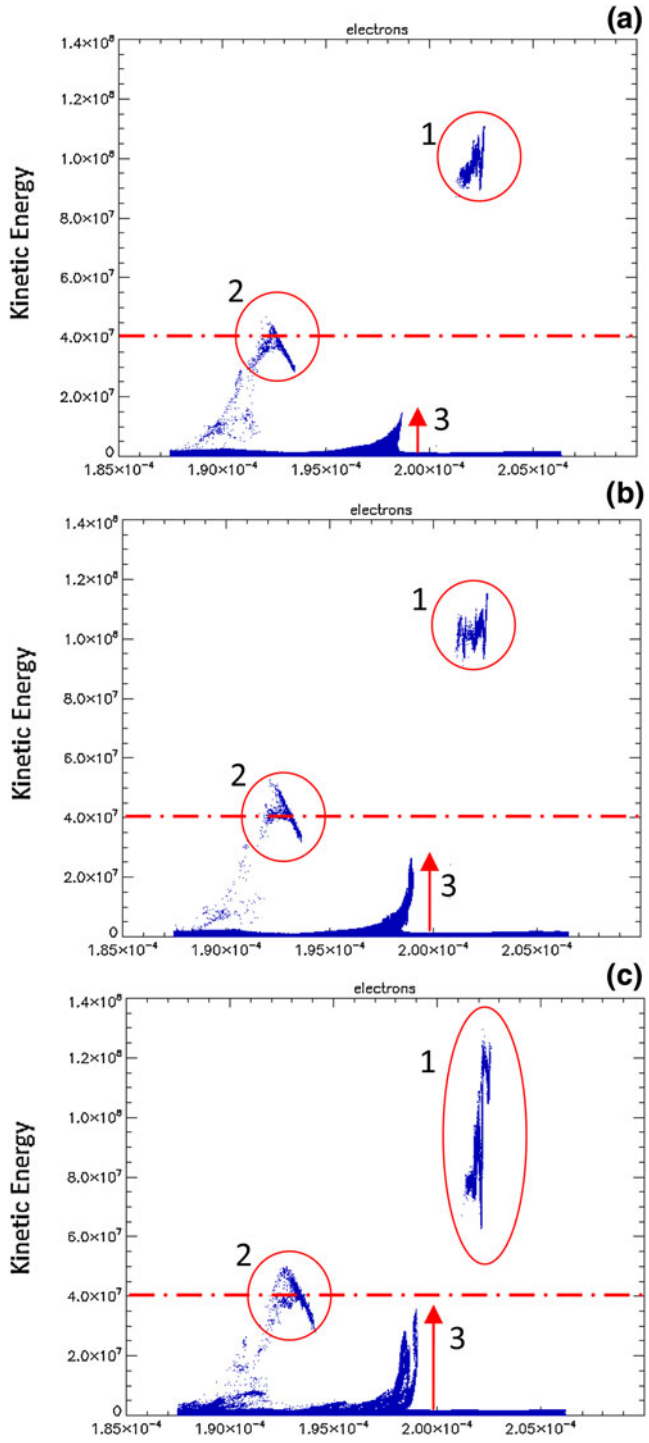

Fig. 3. (Color online) Phase-space diagram for the kinetic energy of electrons in three distinct cases: (**a**) Case-0, Without CNT (**b**) Case-1, $n_{tube} = 30n_0$ (**c**) Case-2, $n_{tube} = 90n_0$. The kinetic energy is given in eV.

https://doi.org/10.1017/S0263034614000433 Published online by Cambridge University Press

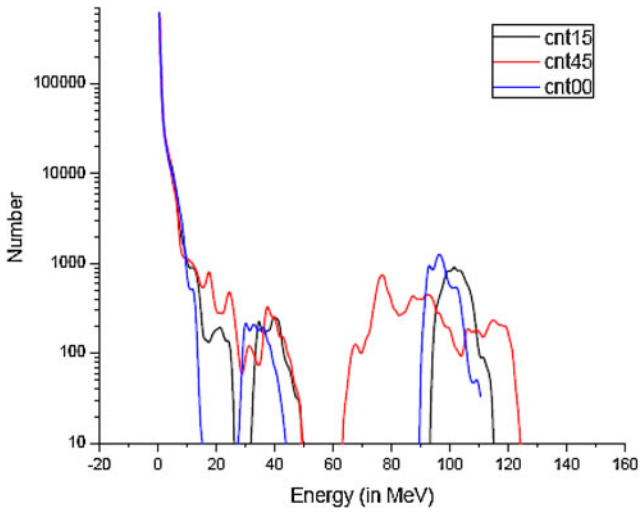

Fig. 4. (Color online) Energy spectrum for three cases: (**a**) Case-1 without CNT (**b**) Case-2 with CNT at $n_{tube} = 30n_0$ (**c**) Case-3 $n_{tube} = 90n_0$.

from the maximum cut-off energy of the bulk electrons (17 MeV) (Fig. 4.). Hence, we obtain two distinct bunches of accelerated electrons in the first two buckets with their characteristic energy gap. We run two more simulations, called case-1 and case-2, using the same set of parameters but introducing a CNT along the laser axis. The thickness of the tube is 25 nm. In case-1, the density inside tube is considered 30 times the background plasma density where as it is 90 times in case-2. The choices restrict the change in the average plasma density to less than 3–4%.

All the three features (depicted by 1, 2, 3, respectively, in Fig. 3) of accelerated electrons in a LWFA show a remarkable shift when a CNT is introduced along the laser axis. In case-1, the entire bunch gains energy by 4–5 % as compared to the reference case-0. The new energy range is (93–115 MeV) instead of (89–111 MeV), showing about a 4% enhancement without any additional energy spread (Fig. 4). However, in case-2, the energy spectrum of the first bubble changes drastically. The bunch energy shows a flattened behavior with reduced number density and enhanced energy spread 63–125 MeV expanding on either side of the spectrum (Fig. 4). The number of accelerated electrons in the bunch is enhanced, though at the expense of energy spread, by merely changing the tube density. The bunch of electrons in the second bubble also experiences an enhanced acceleration due to the tube. The maximum energy cut-off of the second bunch in case-0 is 46 MeV. Due to the presence of tube it reaches up to 54 MeV. The total number of accelerated particles is also enhanced as shown by the enhanced peaks. The gap in the energy spectrum of the two bunches from bubble-1 and bubble-2 remains almost unchanged in case-1 around 40 MeV. However, this gap reduces drastically to about 10 MeV for case-2. The tube has a noticeable effect on the energy of the bulk electrons (Fig. 3a-3). In case-0, the maximum energy cut-off is 15 MeV. This cut-off increases to about 25 MeV for case-1 (Fig. 3b-3) but is still much lower than the lower cut-off of the second bunch . This reduced energy gap is totally vanished for case-2 (Fig. 3c-3). The merged energy spectrum has a combined cut-off at 54 MeV.

We have numerically evaluated and plotted the axial and the transverse electric field profile as given by Eqs. (4) and (5) up to the bunch location (1 μm) from the laser axis. The axial field is strong around the stagnation point (at $x' = 0$) facilitating the additional pull inside the bubble (Fig. 5). The transverse field is strong closer to the axis and gradually becomes weak as one goes away from the laser axis (Fig. 6). One can calculate the average gain as the accelerated bunch remains confined closer to the laser axis. We numerically evaluate the additional gain in the energy of a test electron due to the axial electric field generated by the charged sheet. The numerical value of the additional kinetic energy, following Eq. (6), can be averaged out up to the transverse extent of the bunch as

$$[KE_{add}]_{\text{avg}} = \frac{Z_A N_T e^2 \Delta}{2\epsilon_0 \pi} I_{\text{avg}},$$

where

$$I_{avg} = \sum_1^n \frac{1}{n} \int_\alpha^R \int_0^{2R} \frac{(x - x')dx'}{[(x - x')^2 + y_n^2]^{1/2}} dx$$

and α is the starting point close to the stagnation point but much less than the bubble radius ($< \frac{R}{50}$). The distance from the laser axis y_n ranges from 100 nm to 1 μm. The additional gain is maximum for electrons accelerated in the vicinity of the laser axis and gradually decreases away from it. The additional fractional enhancement in energy due to the tube as compared to the bubble is calculated for a range of

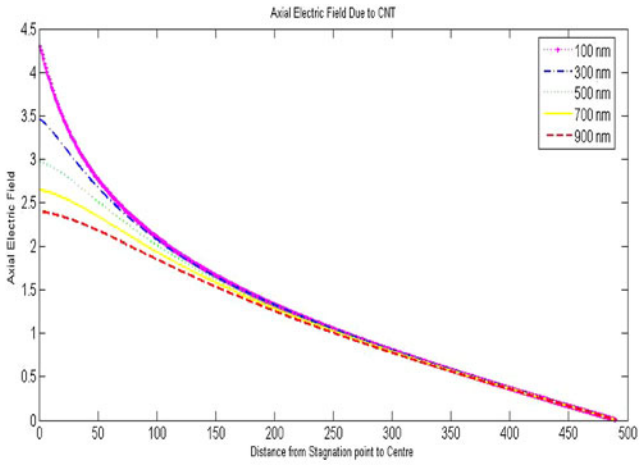

Fig. 5. (Color online) Comparison of axial electrostatic field profile parallel to the laser axis at radial distances: (**i**) 100 nm, (*ii*) 300 nm, (**iii**) 500 nm, (**iv**) 700 nm, and (**v**) 900 nm.

https://doi.org/10.1017/S0263034614000433 Published online by Cambridge University Press

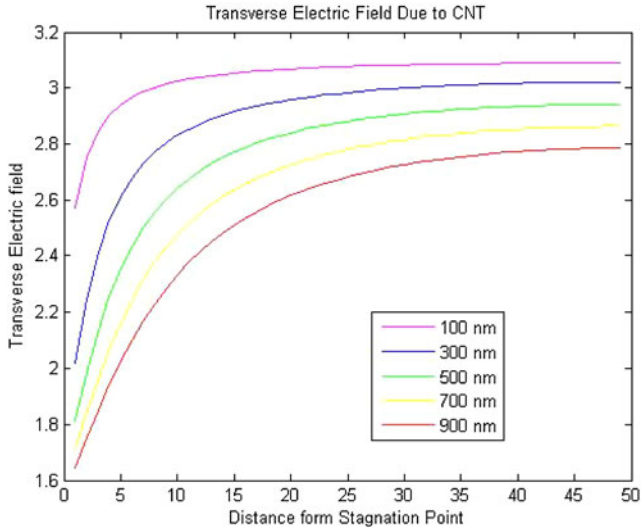

Fig. 6. (Color online) Comparison of transverse electrostatic field profile parallel to the laser axis at distances: (**i**) 100 nm, (**ii**) 300 nm, (**iii**) 500 nm, (**iv**) 700 nm, and (**v**) 900 nm.

practical parameters. For a typical bubble radius $R = 5$ μm, normalized nanotube thickness $\frac{\Delta}{\lambda} = 0.025$, normalized background plasma density $\frac{n_0}{n_{cr}} = 0.01$, one finds that enhancement is about 4–5% for case-1 and about 12–15% for case-2. This is in agreement with the simulation results described above.

4. DISCUSSION

The bubble regime electron acceleration by a short laser pulse in underdense plasma appears to be significantly influenced by the embedded CNT. The immobile charge of the central region affects the goals of LWFA favorably. In all the cases considered, an enhancement in the bunch energy and charge is indicated. The nanometer dimension of the axial high density region changes the average charge density of the plasma only marginally, but it facilitates significant energy enhancement and improves particle confinement in the transverse direction. An equivalent change in the background plasma density doesn't indicate the above benefits. The CNT modifies the electrostatic field (Fig. 5 and Fig. 6) in the bubble most significantly near the axis hence has stronger influence over the electrons pulled from the stagnation point. The spatial location of the CNT relative to the laser axis and its effect on the injection process can be investigated separately as this structure provides a strong field closer to the bubble rear.

ACKNOWLEDGEMENT

The authors are grateful to Prof. C. S. Liu, University of Maryland for his valuable inputs in the present work. The authors acknowledge the financial support from DST, Government of India.

REFERENCES

Bagchi, S., Kiran, P.P., Yang, K., Rao, A.M., Bhuyan, M.K., Krishnamurthy, M. & Kumar, G.R. (2011). Bright, low debris, ultra short hard X-ray table top source using carbon nanotubes. *Phys. Plasmas* **18**, 014502.

Dahiya, D., Sajal, V. & Tripathi, V.K. (2010). Self-injection of electrons in a laser wakefield accelerator by using longitudinal density ripple. *Appl. Phy. Lett.* **96**, 021501.

Davoine, X., Lefebvre, E., Rechatin, C., Faure, J. & Malka, V. (2009). Cold optical injection producing monoenergetic, multi-GeV electron bunches. *Phys. Rev. Lett.* **102**, 065001.

Esarey, E., Hubbard, R.F., Leemans, W.P., Ting, A. & Sprangle, P. (1997). Electron injection into plasma wakefields by colliding laser pulses. *Phys. Rev. Lett.* **79**, 2682.

Faure, J., Glinec, Y., Pukhov, A., Kiselev, S., Gordienko, S., Lefebvre, E., Rousseau, J.P. Burgy, F. & Malka, V. (2004). A laser- plasma accelerator producing monoenergetic electron beams. *Nature London* **431**, 541.

Faure, J., Rechatin, C., Norlin, A., Lifschitz, A., Glinec, Y. & Malik, V. (2006). Controlled injections and acceleration of electrons in plasma wakefields by colliding laser pulses. *Nature* **444**, 737.

Geddes, C.G.R., Toth, C., Tilborg, J.V., Esarey, E., Schroeder, C.B., Bruhwiler, D., Nieter, C., Cary, J. & Leemans, W.P. (2004). High-quality electron beams from a laser wakefield accelerator using plasma channel guiding. *Nature* **431**, 538.

Gu, Y.J., Zhu, Z., Kong, Q., Li, Y.Y., Li, X.F., Chen, C.Y. & Kawata, S. (2011). Laser guiding plasma channel formation criterion in highly relativistic regime. *Appl. Phys. Lett.* **99**, 241501.

Hafz, N.A.M., Jeong, T.M., Choi, I.W., Lee, S.K., Pae, K.H., Kulagin, V.V., Sung, J.H., Yu, T.J., Hong, K.H., Hosokai, T., Vary, J.R., Ko, D.K. & Lee, J. (2008). Stable generation of GeV class electron beams from self-guided laser-plasma channels. *Nat. Photon.* **2**, 571.

Hemker, R.G., Tzeng, K.C., Mori, W.B., Clayton, C.E. & Katsouleas, T. (1998). Computer simulations of cathodeless, high-brightness electron beam production by multiple laser beams in plasmas. *Phys. Rev. E* **57**, 5920.

Hidding, B., Konigstein, T., Osterholz, J., Karsch, S., Willi, O. & Pretzler, G. (2010). Monoenergetic energy doubling in a hybrid laser-plasma wakefield accelerator. *Phys. Rev. Lett.* **104**, 195002.

Hora, H. (2009). Laser fusion with nonlinear force driven plasma blocks: Thresholds and dielectric effects. *Laser Part. Beams* **27**, 207–222.

Jha, P., Saroch, A. & Mishra, A.K. (2013). Wakefield generation and electron acceleration by intense super-Gaussian laser pulses propagating in plasma. *Laser Part. Beams* **31**, 583–588.

Jokar, F. & Eslami, E. (2012). Study of the effect of laser parameters on wakefield excitation in femtoseconds pulsed laser-plasma interaction using PIC method. *Optik* **123**, 1947.

Joshi, C. (2007). The development of laser and beam driven plasma accelerators as an experimental field. *Phys. Plasmas* **14**, 055501.

Kalmykov, S., Yi, S.A., Khudik, V. & Shvets, G. (2009). Electron self-injection and trapping into an evolving plasma bubble. *Phys. Rev. Lett.* **103**, 135004.

Karmakar, A. & Pukkov, A. (2007). Collimated attosecond GeV electron bunches from ionization of high-Z material by radially polarized ultra-relativistic laser pulses. *Laser Part. Beams* **25**, 371–377.

https://doi.org/10.1017/S0263034614000433 Published online by Cambridge University Press

Kostyukov, I., Pukhov, A. & Kiselev, S. (2004). Phenomenological theory of laser-plasma interaction in "bubble" regime. *Phys. Plasmas* **11**, 5256.

Kumar, A., Dahiya, D. & Sharma, A.K. (2011). Laser prepulse induced plasma channel formation in air and relativistic self focusing of an intense short pulse. *Phys. Plasmas* **18**, 023102.

Kumar, K.K. Magesh & Tripathi, V.K. (2012). Laser wakefield bubble regime acceleration of electrons in a preformed non uniform plasma channel. *Laser Part. Beams* **30**, 575–582.

Leemans, W.P., Nagler, B., Gonsalves, A.J., Toth, C., Nakamura, K., Geddes, C.G.R., Esarey, E., Schroeder, C.B. & Hooker, S.M. (2006). GeV electron beams from a centimeter-scale accelerator. *Nat. Phys.* **2**, 696.

Liu, Y., Sheng, Z.M., Zheng, J., Li, F.Y., Xu, X.L., Lu, W., Mori, W.B., Liu, C.S. & Zhang, J. (2012). Ultrafast XUV emission from laser wakefields in underdense plasma. *New J. Phys.* **14**, 083031.

Lu, W., Huang, C., Zhou, M., Mori, W.B. & Katsouleas, T. (2006). Non linear theory for relativistic plasma wakefields in the blowout regime. *Phys. Rev. Lett.* **96**, 165002.

Ma, Y.Y., Sheng, Z.M., Li, Y.T., Chang, W.W. & Yuan, X.H. (2006). Dense quasi-monoenergetic attosecond electron bunches from laser interaction with wire and slice targets. *Phys. Plasmas* **13**, 110702.

Mangles, S.P.D., Murphy, Z.N.C.D., Thomas, J.L.C.A.G.R., Dangor, A.E., Divall, E.J., Foster, P.S., Gallacher, J.G., Hooker, C.J., Jaroszynski, D.A., Langley, A.J., Mori, W.B., Norreys, P.A., Tsung, F.S., Viskup, R., Walton, B.R. & Krushelnick, K. (2004). Monoenergetic beams of relativistic electrons from intense laser-plasma interactions. *Nature (London)* **431**, 535.

Martins, S.F., Fonseca, R.A., Lu, W., Mori, W.B. & Silva, L.O. (2010). Exploring laser-wakefield accelerator regimes for near term lasers using particle-in-cell simulation in Lorentz-boosted frames. *Nat. Phys.* **6**, 311.

Mirzanejhad, S., Sohbatzadeh, F., Asri, M. & Ghanbari, K. (2010). Quasi monoenergetic GeV electron bunch generation by the Wakefield of the chirped laser pulse. *Phys. Plasmas* **17**, 033103.

Miura, E., Koyama, K., Kato, S., Saito, N., Adachi, M., Kawada, Y., Nakamura, T. & Tanimoto, M. (2005). Demonstration of quasi-monoenergetic electron beam generation in laser driven plasma acceleration. *Appl. Phys. Lett.* **86**, 251501.

Murakami, M. & Tanaka, M. (2013). Generation of high quality mega-electron volt proton beams with intense-laser-driven nanotube accelerator. *Appl. Phys. Lett.* **102**, 163101.

Rao, B.S., Chakera, J.A., Naik, P.A., Kumar, M. & Gupta, P.D. (2011). Laser wakefield acceleration in pre-formed plasma channel created by pre-pulse pedestal of terawatt laser pulse. *Phys. Plasmas* **18**, 093104.

Shen, B., Li, Y., Nemeth, K., Shang, H. & Chae, Y.C. (2007). Electron injection by a nanowire in the bubble regime. *Phys. Plasmas* **14**, 053115.

Tajima, T. & Dawson, J.M. (1979). Laser electron accelerator. *Phys. Rev. Lett.* **43**, 267–270.

Uhm, H.S., Nam, I.H., Kur, M.S. & Suk, H. (2013). Large transverse motion and micro-bunching of trapped electrons in a wakefield accelerator driven by temporally-asymmetric laser pulses. *Current Appl. Phys.* **13**, 645–651.

Umstadter, D., Kim, J.K. & Dodd, E. (1996). Laser injection of ultrashort electron pulses into wakefield plasma waves. *Phys. Rev. Lett.* **76**, 2073.

Upadhyay, A.K., Samant, S.A. & Krishnagopal, S. (2013). Tailoring the laser pulse shape to improve the quality of the self-injected electron beam in laser wakefield acceleration. *Phys. Plasmas* **20**, 013106.

Vieira, J., Martins, S.F., Pathak, V.B., Fonseca, R.A., Mori, W.B. & Silwa, L.O. (2011). Magnetic control of particle injection in plasma based accelerators. *Phys. Rev. Lett.* **106**, 225001.

Vieira, J., Martins, J.L., Pathak, V.B., Fonseca, R.A., Mori, W.B. & Silva, L.O. (2012). Magnetically assisted self-injection and radiation generation for plasma based acceleration. *Plasma Phys. Contr. Fusion* **54**, 124044.

Wang, W.M., Sheng, Z.M. & Zhang, J. (2008). Controlled electron injection into laser wakefields with a perpendicular injection laser pulse. *Appl. Phys. Lett.* **93**, 201502.

Xu, J., Shen, B., Zhang, X., Wen, M., Ji, L., Wang, W., Yu, Y. & Nakajima, K. (2010). Generation of a large amount of energetic electrons in complex structure bubble. *N. J. of Physics* **12**, 023037.

Yi, S.A., Khudik, V., Siemon, C. & Shvets, G. (2013). Analytical model of electromagnetic fields around a plasma bubble in the blow out regime. *Phys. Plasmas* **20**, 013108.

Zhang, L., Chen, L.M., Wang, W.M., Yan, W.C., Yuan, D.W., Mao, J.Y.,Wang, Z., Liu, C., Shen, Z.W., Faenov, A., Pikuz, T., Li, D.Z., Li, Y.T., Dong, Q.L., Lu, X., Ma, J.L., Wei, Z.Y., Sheng, Z.M. & Zhang, J. (2012). Electron acceleration via high contrast laser interacting with submicron clusters. *Appl. Phy. Lett.* **100**, 014104.

https://doi.org/10.1017/S0263034614000433 Published online by Cambridge University Press